UNIFAC Model for Ionic Liquid-CO (H_2) Systems: An Experimental and Modeling Study on Gas Solubility

Zhigang Lei, Chengna Dai, Qian Yang, Jiqin Zhu, and Biaohua Chen
State Key Laboratory of Chemical Resource Engineering, Beijing University of Chemical Technology, Box 266, Beijing 100029, China

DOI 10.1002/aic.14606
Published online September 2, 2014 in Wiley Online Library (wileyonlinelibrary.com)

The universal quasichemical functional-group activity coefficients (UNIFAC) model for ionic liquids (ILs) has become notably popular because of its simplicity and availability via modern process simulation softwares. In this work, new group binary interaction parameters (α_{mn} and α_{nm}) between CO (H_2) and IL groups were obtained by correlating the solubility data in pure ILs at high temperatures (above 273.2 K) collected from the literature. the solubility of CO in $[BMIM]^+[BF_4]^-$, $[OMIM]^+[BF_4]^-$, $[OMIM]^+[Tf_2N]^-$, and their mixtures, as well as that of H_2 in $[EMIM]^+[BF_4]^-$, $[BMIM]^+[BF_4]^-$, $[OMIM]^+[Tf_2N]^-$, and their mixtures, at temperatures from 243.2 to 333.2 K and pressures up to 6.0 MPa were measured. The UNIFAC model was observed to well predict the solubility in pure and mixed ILs at both high (above 273.2 K) and low (below 273.2 K) temperatures. Moreover, the selectivity of CO (or H_2) to CO_2 in ILs increases with decreasing temperature, indicating that low temperatures favor for gas separation. © 2014 American Institute of Chemical Engineers *AIChE J*, 60: 4222–4231, 2014

Keywords: universal quasichemical functional-group activity coefficients model, CO solubility, H_2 solubility, selectivity, ILs, low temperatures

Introduction

In recent years, ionic liquids (ILs) have attracted increasing attention as novel green solvents because of their unique properties,[1–3] such as nonvolatility at temperatures near room temperature, tunable properties by the proper choice of chemical structures, high thermal, and chemical stability, and low-melting points, which make them candidates to replace traditional organic solvents in different chemical processes.[4–15] For example, in the current Rectisol process for capturing CO_2 from syngas, methanol acts as a separating agent. However, it is highly volatile, which leads to the incorporation of a complicated and energy-intensive system for recovering the methanol entrained at the top of the absorption column. Thus, ILs are an attractive alternative to methanol in the Rectisol process. The task of capturing CO_2 from syngas is so strict that the absorption column in the Rectisol process with methanol as the solvent must be operated at temperatures as low as 243 K to ensure high solubility and selectivity. A typical feed composition of syngas (mole percentage) is as follows: H_2 32.31, CO_2 15.25, CO 44.44, CH_4 1.88, and H_2S 86.32 ppm.[16] After absorption, the CO_2 content in syngas is limited to the ppm level at the top of the absorption column.[17,18] Evidently, the key components should be focused on H_2, CO, and CO_2 in terms of the required separation task and the given gas composition. For a better understanding of the thermodynamic behavior of IL-gas systems, reliable solubility data of gases in ILs covering a wide temperature range are necessary.

Unfortunately, although the literature contains a huge number of solubility data of CO_2 in ILs, even including data collected at low temperatures down to 228 K, the solubility data of CO or H_2 in ILs are very limited, involving approximately 200 and 600 data points for IL-CO[19–30] and IL-H_2 systems,[27–41] respectively. Furthermore, no solubility data for CO or H_2 in ILs at low temperatures (below 273.2 K) have been reported thus far. This paucity of data is partly because CO and H_2 are sparingly soluble in most common ILs; thus, their solubility is relatively difficult to measure with sufficient precision. In this case, we should resort to the predictive thermodynamic models, which can predict the thermodynamic properties of systems of interest, especially under extreme conditions (e.g., low temperatures and high pressures) to reduce the amount of experimental work required. It is generally believed that both the conductor-like screening model for real solvents (COSMO-RS) and universal quasichemical functional-group activity coefficients (UNIFAC) models are efficient predictive methods. However, the COSMO-RS model often provides a qualitative description of thermodynamic behavior of the systems containing ILs, whereas the UNIFAC model can give quantitatively correct prediction.[8,42] For process simulation, design and optimization, in most cases only qualitative prediction is not sufficient. Moreover, the UNIFAC parameters can be directly applied to the modern process simulation softwares such as PROII, Aspen Plus, and ChemCAD to establish the equilibrium-stage (EQ) and nonequilibrium-stage (NEQ)

Additional Supporting Information may be found in the online version of this article.

Correspondence concerning this article should be addressed to Z. Lei at leizhg@mail.buct.edu.cn

© 2014 American Institute of Chemical Engineers

mathematical models. As a result, the UNIFAC model for ILs has been widely applied in the community of chemical engineering.[43,44] Very recently, the UNIFAC model was extended to IL-CO_2 systems; however, the group parameters between IL and CO (H_2) systems have not yet been included in the current UNIFAC parameter matrix.[45]

To speedup the application of the new technology of capturing CO_2 with ILs at low temperatures, the focus of this work is on addressing the fundamental issues regarding the UNIFAC model to (1) add new group parameters between ILs and CO (H_2) into the UNIFAC parameter matrix by correlating the solubility data exhaustively collected from literature, where the data covers different pressures and high temperatures (above 273.2 K); (2) verify the applicability of the UNIFAC model for predicting the solubility of CO (H_2) in pure ILs from high to low temperatures (below 273.2); (3) determine whether the UNIFAC model can be extrapolated to predict the solubility of CO (H_2) in mixed ILs (MILs); and (4) identify the structure–property relation for CO and H_2 solubility in ILs, and thus, understand the advantages of capturing CO_2 with ILs at low temperatures. For this purpose, the solubility of CO at temperatures down to 243.2 K and pressures up to 6.0 MPa was measured in three common ILs, that is, $[BMIM]^+[BF_4]^-$, $[OMIM]^+[BF_4]^-$, and $[OMIM]^+[Tf_2N]^-$, and their binary mixtures ($[OMIM]^+[BF_4]^- + [OMIM]^+[Tf_2N]^-$), in this work. Because of the inverse temperature effect, the solubility of H_2 in ILs would be much smaller at low temperatures (below 273.2 K); thus, in this case, an experimental apparatus with high accuracy is required. In this work, H_2 solubility was not measured at low temperatures, but at two high temperatures (313.2 and 333.2 K) and pressures up to 6.0 MPa in three ILs ($[EMIM]^+[BF_4]^-$, $[BMIM]^+[BF_4]^-$, and $[OMIM]^+[Tf_2N]^-$) and their binary mixtures ($[EMIM]^+[BF_4]^- + [OMIM]^+[Tf_2N]^-$, and $[BMIM]^+[BF_4]^- + [OMIM]^+[Tf_2N]^-$). The use of MILs serves to multiply the possibilities of tuning the desirable solubility and selectivity in gas separation rather than through complicated chemical synthesis of single ILs. The meaning of abbreviations and structures for the cations and anions of ILs used throughout this article are presented in Supporting Information Table S1.

Experimental Section

Materials

The ILs $[EMIM]^+[BF_4]^-$ (molecular mass 197.97 $g \cdot mol^{-1}$, purity > 99%, water content <2000 ppm, and chloride content <300 ppm in mass fraction), $[BMIM]^+[BF_4]^-$ (molecular mass 226.02 $g \cdot mol^{-1}$, purity >99 %, water content <2000 ppm, and chloride content <200 ppm in mass fraction), $[OMIM]^+[BF_4]^-$ (molecular mass 282.13 $g \cdot mol^{-1}$, purity >99 %, water content <2000 ppm, and chloride content <150 ppm in mass fraction), $[HMIM]^+[Tf_2N]^-$ (molecular mass 447.43 $g \cdot mol^{-1}$, purity >99 %, water content <2000 ppm, and chloride content <200 ppm in mass fraction) and $[OMIM]^+[Tf_2N]^-$ (molecular mass 475.47 $g \cdot mol^{-1}$, purity >99 %, water content <600 ppm, and chloride content <150 ppm in mass fraction), were purchased from Shanghai Chengjie Chemical Co. Before use, they were preprocessed at 333.2 K for 24 h in a vacuum rotary evaporator to remove traces of water and other volatile impurities. The water contents in ILs after rotary evaporation (but before solubility experiments) were less than 400 ppm, as determined by the Karl Fischer titration method (SC-6), which was calibrated using 0.1 μL of distilled water beforehand. H_2 (purity >99.99 wt %) and CO (purity >99.99 wt %) were purchased from Beijing Longkou City Gas Plant and were used without further purification.

Apparatus and procedure

The solubility of CO in ILs at temperatures below 293.2 K was measured using a low-temperature equilibrium apparatus, the details of which have been described in our previous publication.[46] In this apparatus, the temperature was controlled with cooling ethanol with a fluctuation of ±0.1 K, and the system pressure was measured by a pressure gauge with a range of 0–9.999 MPa and a fluctuation of ±0.001 MPa. Conversely, the solubility of CO at temperatures above 293.2 K and the solubility of H_2 at temperatures of 313.2 and 333.2 K were measured using a high-temperature and high-pressure view-cell apparatus, the details of which have been described in our previous publications.[47–49] The temperature was controlled by electric heating elements with a fluctuation of ±0.1 K, and the system pressure was measured by a pressure gauge with a range of 0–20.00 MPa and a fluctuation of ±0.01 MPa.

In a typical experiment, a certain amount of IL was first loaded into the equilibrium cell, which was evacuated with a vacuum pump (2XZ-1) to purge the air from the system. The equilibrium cell was then purged with CO (or H_2) several times. Afterward, a charge of CO (or H_2) was introduced into the equilibrium cell. When gas dissolved into the IL, the pressure decreased gradually. The IL phase was mixed with a stirring paddle at a stirring speed of approximately 200 rpm. After the gas-liquid equilibrium was reached as indicated by negligible temperature and pressure changes, a small amount of liquid sample (approximately 1.5–2.0 g) was collected and transferred to a sample bomb. The amounts of IL and dissolved gas in the liquid sample were determined using the drainage gas-collecting method, that is, the dissolved gas was released slowly from the sample bomb into a buffer bottle filled with deionized water. Thus, the gas amount was derived by weighing the water mass discharged. Meanwhile, the IL amount was determined using the gravimetric method by measuring the mass difference of the liquid sample with and without gas. Masses were measured on an electronic balance (CPA 1003S, Sartorius) with an uncertainty of 0.001 g. Notably, during the measurement, it was assumed that no IL appeared in the gas phase.[50] Under the same temperature and pressure, each experiment was conducted at least three times to ensure the reproducibility of experimental data. In this way, the uncertainties of H_2 solubility were estimated to be less than 0.0030 in mole fraction, whereas the uncertainties of CO solubility at low and high temperatures were estimated to be less than 0.0030 and 0.0020 in mole fraction, respectively, as deduced from error propagation calculations.

It should be noticed that we do not report the solubility data of H_2 in ILs at low temperatures in this work, because H_2 solubility exhibits a so-called "inverse" temperature effect.[34] In contrast to CO and CO_2 solubility, H_2 solubility tends to decrease at low temperatures. In this case, it is difficult to collect the viscous liquid sample from the equilibrium cell because the low-H_2 solubility at low temperatures cannot counteract the increase in viscosity of the IL in the mixture.

The accuracy and reliability of the experimental apparatus and procedure were validated by comparing the experimental

solubility data of CO at 293.3 K in $[HMIM]^+[Tf_2N]^-$ and H_2 at 313.05 K in $[BMIM]^+[PF_6]^-$ with the results reported in the literature.[24,31] It was found that the average relative deviations (ARDs) were 7.71% for $[HMIM]^+[Tf_2N]^-$ (Ref. 24) and 3.74% for $[BMIM]^+[PF_6]^-$ (Ref. 31), respectively (Figures S1 and S2 in Supporting Information for more details). However, we are aware that the deviation of experimental data between this work and the literature (Ref. 24) for $[HMIM]^+[Tf_2N]^-$—CO system becomes a little large at high-pressure region, while the solubility data reported by Maurer's research group are thought to be among the most accurate. This may be mainly due to the operation difficulties at elevated pressures for toxic gases like CO, other than different experimental techniques and sample sources used in the solubility measurement.

Thermodynamic Model

Model description

In the UNIFAC model for ILs, the activity coefficient γ_i is calculated by the sum of the following two terms:

$$\ln \gamma_i = \ln \gamma_i^C + \ln \gamma_i^R \quad (1)$$

where $\ln \gamma_i^C$ represents the combinatorial contribution to the activity coefficient and $\ln \gamma_i^R$ represents the residual contribution. The $\ln \gamma_i^C$ term, given the effect of differences in the sizes and shapes of groups, contains two parameters: the group volume parameter R_k and the group surface area Q_k, both of which can be obtained via the COSMO calculation.[51,52] In this work, $R_k(CO) = 1.047$; and $Q_k(CO) = 1.060$; $R_k(H_2) = 0.528$; and $Q_k(H_2) = 0.664$, as calculated by the COSMO-RS model (ADF version).[53,54]

The $\ln \gamma_i^R$ term contains the group interaction parameters (α_{mn} and α_{nm}). Fortunately, the group interaction parameters (α_{mn} and α_{nm}) between the IL group and the main group CH_2 are available from previous publications.[41,42] When the UNIFAC model was used to predict the solubility of gases in binary mixed ILs, the binary interaction parameters between two IL groups were assumed to be zero because they exhibit similar polarity. However, the group interaction parameters (α_{mn} and α_{nm}) between the CO (H_2) group and the main group CH_2, as well as those between the IL and CO (H_2) groups, are the unknown input parameters, which should be derived by correlating the experimental CO (H_2) solubility data in pure alkanes and in ILs at different temperatures (above 273.2 K) and pressures. For alkane-CO (H_2) systems, the data source is the book titled "Solubility of Gases in Liquids" edited by Fogg and Gerrard,[55] whereas, for IL-CO (H_2) systems, the solubility data were exhaustively collected from literature published by the end of May 2014. All the solubility data have been converted to the mole-fraction basis and are listed in Supporting Information Tables S2 and S3.

Table 1. Group Binary Interaction Parameters α_{mn} and α_{nm} for the UNIFAC Model

m	*n*	α_{mn}	α_{nm}
H_2	CH_2	42.0822	496.4461
	$[MIM][BF_4]$	865.7954	641.1374
	$[MIM][PF_6]$	1084.5745	1649.1892
	$[MIM][Tf_2N]$	726.1560	998.6247
	$[MPY][Tf_2N]$	427.1756	1038.6811
CO	CH_2	42.8215	140.1621
	$[MIM][BF_4]$	361.3960	645.0209
	$[MIM][MeSO_4]$	2212.6707	2507.3187
	$[MIM][PF_6]$	468.2990	685.1949
	$[MIM][Tf_2N]$	188.3112	345.4088

Procedure for estimating group interaction parameters

For gas (1)—IL (or high-boiling point solvent) and (2) binary systems, the gas-liquid equilibrium at low and medium pressures is written as

$$y_1 P \phi_1(T, P, y_1) = x_1 \gamma_1 P_1^s \quad (2)$$

where x_1 and y_1 represent the mole fractions of CO (H_2) in the liquid and gas phases, respectively; $\phi_1(T, P, y_1)$ is the fugacity coefficient of CO (H_2) in the gas phase, as calculated using the Peng–Robinson (PR) equation; P is the system pressure; P_1^s is the saturated vapor pressure of CO (H_2) calculated by the extrapolated Antoine equation obtained from the book edited by Fogg and Gerrard[55]; and γ_1 is the activity coefficient of CO (H_2) in the liquid phase, as calculated by the UNIFAC model. Because of the large difference

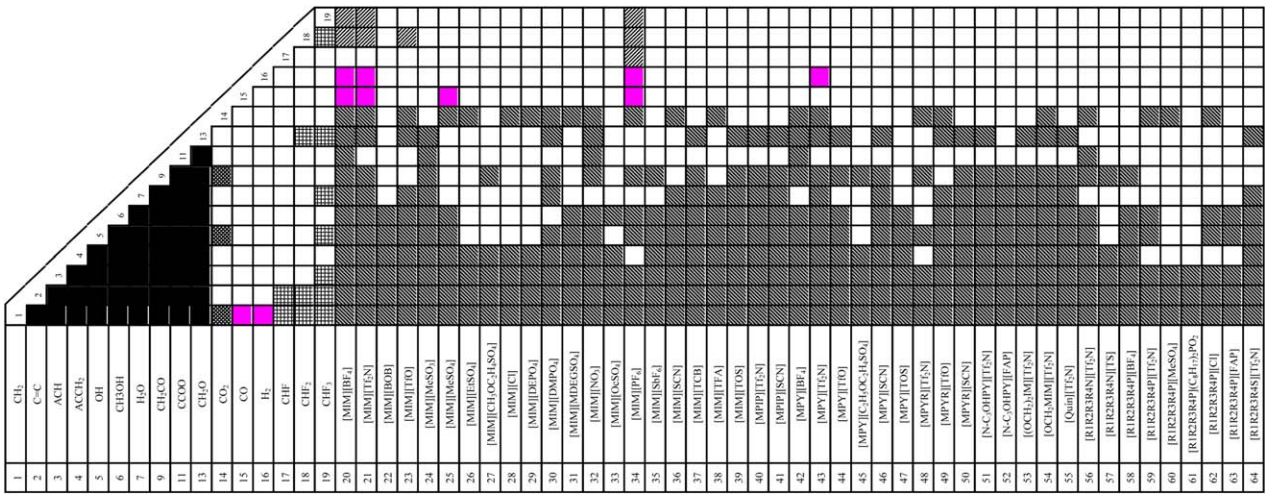

Figure 1. Current UNIFAC parameter matrix for ILs.

■ Previously published parameters;[62] ▧ parameters previously published by our group;[43–45,] ▨ previously published parameters;[60] ▦ previously published parameters;[63] ▩ previously published parameters;[64] ■ new parameters (this work); □ no parameters available. [Color figure can be viewed in the online issue, which is available at wileyonlinelibrary.com.]

Table 2. Comparison of Experimental CO and H_2 Solubility in ILs with the Results Predicted by the UNIFAC Model

IL–gas systems	T range (K)	P range (bar)	ARD (%)	No. of data points	Refs.
$[BMIM]^+[BF_4]^-$–CO	283.18–343.04	0.80–0.90	5.19	9	21
$[BMIM]^+[MeSO_4]^-$–CO	293.15–413.15	12.71–93.31	35.22	25	29
$[BMIM]^+[PF_6]^-$–CO	293.20–373.15	7.68–91.67	12.19	36	23
	283.16–343.27	0.81–0.91	42.46	8	27
$[BMIM]^+[Tf_2N]^-$–CO	309.19–458.15	47.85–103.43	17.56	44	19
$[HMIM]^+[Tf_2N]^-$–CO	293.20–413.15	14.59–97.85	14.52	24	24
	300.70–437.29	40.49–116.72	8.72	45	26
	313.15–433.15	40.82–112.55	9.15	16	26
		Total	16.26	207	
$[BMIM]^+[BF_4]^-$–H_2	278.20–343.11	0.43–0.90	24.02	16	21
$[BMIM]^+[PF_6]^-$–H_2	283.40–343.14	0.45–0.92	34.30	15	27
	313.05–373.15	10.84–91.00	36.92	32	31
$[BMIM]^+[Tf_2N]^-$–H_2	313.48–453.15	26.76–154.34	9.42	100	34
	283.45–343.13	0.75–0.92	32.12	11	36
$[BMPY]^+[Tf_2N]^-$–H_2	293.00–413.00	14.72–82.72	6.77	24	33
$[EMIM]^+[PF_6]^-$–H_2	298.00–356.40	26.82–32.51	8.99	6	35
$[EMIM]^+[Tf_2N]^-$–H_2	282.98–343.07	0.45–0.90	52.78	13	37
	312.14–452.42	57.14–143.05	12.12	52	38
$[HMIM]^+[Tf_2N]^-$–H_2	283.88–343.02	0.78–0.94	23.93	11	39
	293.15–368.41	45.79–118.53	8.11	83	36
	293.20–413.20	14.76–98.19	8.97	25	32
		Total	15.64	388	

in boiling point between the gas and IL (or high-boiling point solvent), the gas phase can be treated as a pure gas component (i.e., $y_1 = 0$).[50]

The ARD minimized as objective function (OF) was used to obtain the group interaction parameters (α_{mn} and α_{nm}):

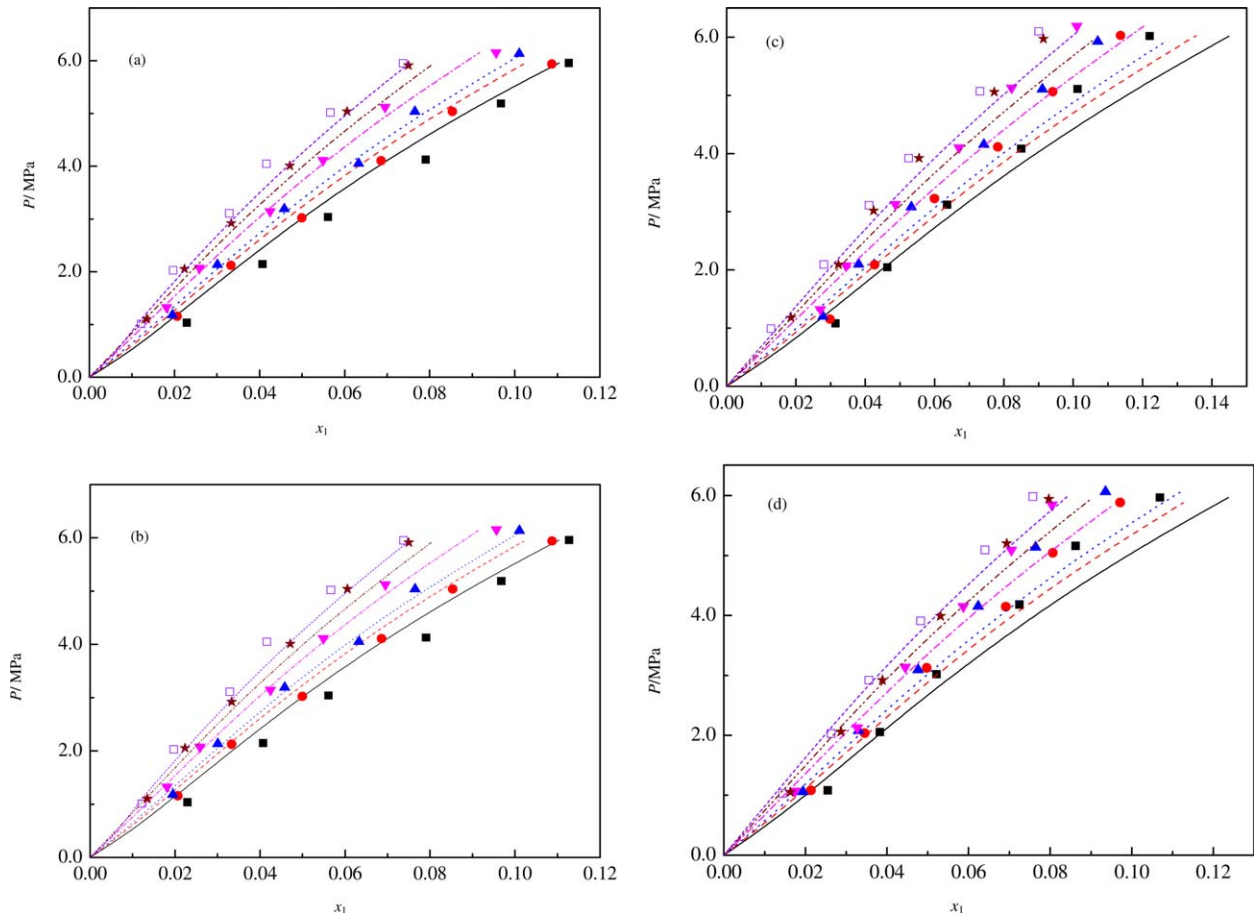

Figure 2. Solubility of CO in pure $[BMIM]^+[BF_4]^-$ (a), $[OMIM]^+[BF_4]^-$ (b), $[OMIM]^+[Tf_2N]^-$ (c), and in binary mixture of 50 wt % $[OMIM]^+[BF_4]^-$ + 50 wt % $[OMIM]^+[Tf_2N]^-$ (d).

Lines, results predicted by the UNIFAC model; scattered points, experimental data. (■) and (——) 243.2 K; (●) and (– – –) 258.2 K; (▲) and (·····) 268.2 K; (▼) and (–·–) 293.2 K; (★) and (–··–) 313.2 K; (□) and (- - - -) 333.2 K. [Color figure can be viewed in the online issue, which is available at wileyonlinelibrary.com.]

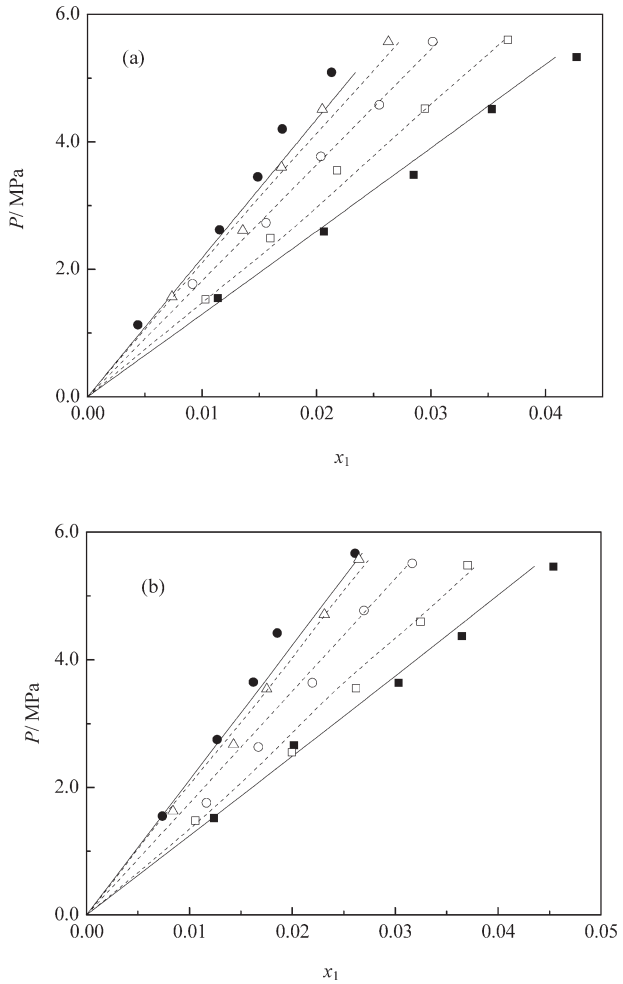

Figure 3. Solubility of H_2 in $[EMIM]^+[BF_4]^-$, $[OMIM]^+[Tf_2N]^-$, and their mixtures at 313.2 K (a) and 333.2 K (b).

Solid lines, results predicted by the UNIFAC model for pure ILs; dashed lines, results predicted by the UNIFAC model for binary mixtures of ILs; scattered points, experimental data. (■) $[OMIM]^+[Tf_2N]^-$; (□) 20 wt % $[EMIM]^+[BF_4]^-$ + 80 wt % $[OMIM]^+[Tf_2N]^-$; (○) 50 wt % $[EMIM]^+[BF_4]^-$ + 50 wt % $[OMIM]^+[Tf_2N]^-$; (△) 80 wt % $[EMIM]^+[BF_4]^-$ + 20 wt % $[OMIM]^+[Tf_2N]^-$; (•) $[EMIM]^+[BF_4]^-$. [Color figure can be viewed in the online issue, which is available at wileyonlinelibrary.com.]

$$\mathrm{OF}=\min\left\{\frac{1}{N}\sum_{1}^{N}\left|\frac{x_{\mathrm{cal}}-x_{\mathrm{exp}}}{x_{\mathrm{exp}}}\right|\right\} \tag{3}$$

where x_{exp} is the experimental CO (H_2) solubility data collected from the literature; x_{cal} is the CO (H_2) solubility data calculated using the UNIFAC model; and N is the number of data points.

The estimation of the group interaction parameters (α_{mn} and α_{nm}) was conducted in a sequential fashion, that is, the parameters between CO (H_2) and the main group CH_2 were first regressed using the experimental data for alkane-CO (H_2) systems. These values were subsequently used to obtain the parameters between the IL and CO (H_2) groups. In this work, the IL molecule was decomposed into several functional groups in a manner similar to that adopted by Lei and coworkers,[43–46] Kim et al.,[56,57] Breure et al.,[58] and others.[59–61] The fitting procedure using the SOLVER function in Microsoft Excel 2007 to obtain the group binary interaction parameters is similar to that used in our previous publications, where the optimization algorithm of Newton's central difference was chosen. As a result, the group interaction parameters (α_{mn} and α_{nm}) between the CO (H_2) group and the main group CH_2, as well as those between the CO (H_2) group and IL groups, are listed in Table 1. The UNIFAC parameter matrix for the ILs is illustrated in Figure 1. Notably, the group parameters available from the literature remain unchanged. All of the investigated ILs, data points, experimental measurement methods, and the corresponding literature are given in detail in Supporting Information.

Results and Discussion

Prediction of the solubility of CO in pure and mixed ILs from high to low temperatures

The experimental CO solubility data at high temperatures and the results calculated by the UNIFAC model are

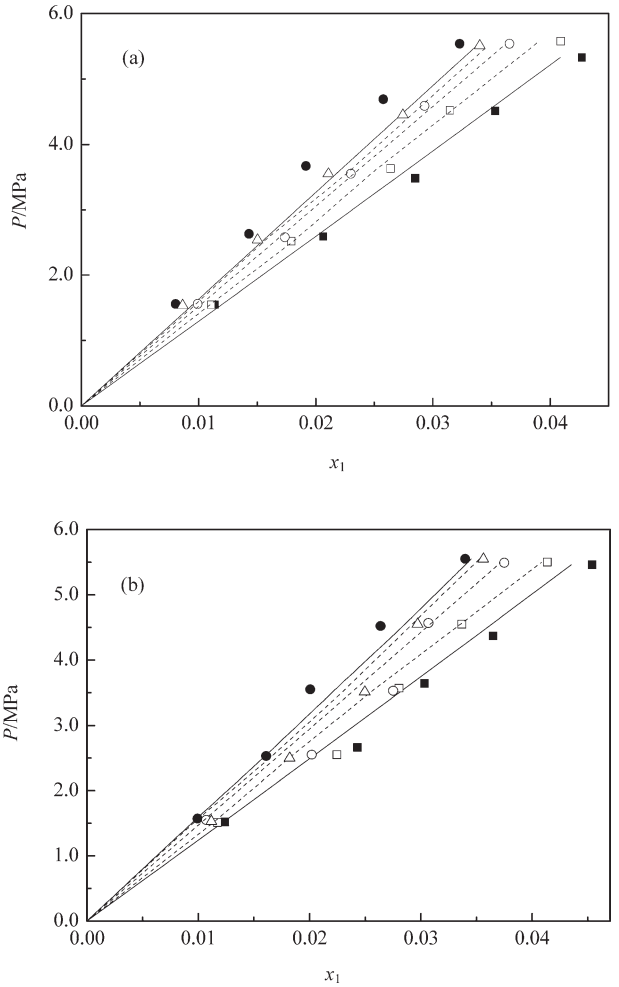

Figure 4. Solubility of H_2 in $[BMIM]^+[BF_4]^-$, $[OMIM]^+[Tf_2N]^-$, and their mixtures at 313.2 K (a) and 333.2 K (b).

Solid lines, results predicted by the UNIFAC model for pure ILs; dashed lines, results predicted by the UNIFAC model for binary mixtures of ILs; scattered points, experimental data. (■) $[OMIM]^+[Tf_2N]^-$; (□) 20 wt % $[EMIM]^+[BF_4]^-$ + 80 wt % $[OMIM]^+[Tf_2N]^-$; (○) 50 wt % $[EMIM]^+[BF_4]^-$ + 50 wt % $[OMIM]^+[Tf_2N]^-$; (△) 80 wt % $[EMIM]^+[BF_4]^-$ + 20 wt % $[OMIM]^+[Tf_2N]^-$; (•) $[EMIM]^+[BF_4]^-$.

Table 3. Henry's Constant of CO in ILs Determined Experimentally (H_{exp}) and Predicted by UNIFAC (H_{pre}) at Different Temperatures (the Values in Parenthesis Come from the Lever Rule)

ILs	T (K)	H_{exp} (MPa)	H_{pre} (MPa)	RD
$[BMIM]^+[BF_4]^-$	333.2	167.63	162.24	0.0322
	313.2	148.04	147.23	0.0055
	293.2	130.51	131.69	0.0091
	268.2	104.35	111.67	0.0702
	258.2	101.08	103.53	0.0243
	243.2	88.31	91.26	0.0335
$[OMIM]^+[BF_4]^-$	333.2	96.73	90.23	0.0672
	313.2	91.76	81.45	0.1123
	293.2	77.82	72.48	0.0685
	268.2	65.22	61.07	0.0636
	258.2	60.35	56.48	0.0641
	243.2	54.82	49.60	0.0952
$[OMIM]^+[Tf_2N]^-$	333.2	70.29	67.26	0.0431
	313.2	66.46	60.53	0.0892
	293.2	63.05	53.72	0.1480
	268.2	50.99	45.17	0.1141
	258.2	38.66	41.76	0.0802
	243.2	37.42	36.69	0.0195
50 wt % $[OMIM]^+[BF_4]^-$	333.2	79.49	80.32 (81.68)	0.0105 (0.0275)
+ 50 wt % $[OMIM]^+[Tf_2N]^-$	313.2	74.51	72.31 (73.66)	0.0295 (0.0114)
	293.2	71.25	64.17 (65.49)	0.0994 (0.0808)
	268.2	64.37	53.89 (55.15)	0.1628 (0.1433)
	258.2	59.94	49.77 (51.00)	0.1697 (0.1492)
	243.2	54.77	43.63 (44.79)	0.2034 (0.1822)

compared in Table 2. As a whole, the results calculated by the UNIFAC model are similar to the experimental data reported in the literature. To test the predictive power of the UNIFAC model, the solubility data of CO at temperatures as low as 243.2 K in three common ILs, that is, $[EMIM]^+[BF_4]^-$, $[BMIM]^+[BF_4]^-$, and $[OMIM]^+[Tf_2N]^-$, measured in this work were used as "test set" and were compared with the values predicted by the UNIFAC model. Figures 2a–c show the experimental solubility of CO at temperatures from 243.2 to 333.2 K and pressures up to 6.0 MPa in pure $[BMIM]^+[BF_4]^-$, $[OMIM]^+[BF_4]^-$, and $[OMIM]^+[Tf_2N]^-$, along with the results predicted by the UNIFAC model, where x_1 represents the mole fraction of CO in the IL. It can be seen that CO solubility increases with decreasing temperature. Moreover, the UNIFAC model can well predict the CO solubility in pure ILs at both high and low temperatures. The ARDs for $[BMIM]^+[BF_4]^-$, $[OMIM]^+[BF_4]^-$, and $[OMIM]^+[Tf_2N]^-$ are 6.49%, 6.35%, and 11.83%, respectively, thereby verifying the applicability of the UNIFAC model for predicting CO solubility in pure ILs from high to low temperatures. The detailed solubility data of CO in pure ILs are listed in Supporting Information Table S4.

Figure 2d shows the experimental and predicted results of CO solubility in binary mixed ILs of 50 wt % $[OMIM]^+[BF_4]^-$ + 50 wt % $[OMIM]^+[Tf_2N]^-$ (on a CO-free basis) at temperatures from 243.2 to 333.2 K. The ARD between experimental and predicted data is 9.55%, indicating that the UNIFAC model can predict the solubility of CO in binary mixed ILs efficiently at both high and low temperatures.

Prediction of the solubility of H_2 in pure and mixed ILs

The experimental H_2 solubility data collected at high temperatures obtained from the literature and the results calculated by the UNIFAC model are summarized in Table 2. In most cases, the experimental data and calculated results agree. However, the ARDs for H_2 and CO gas are greater than those for CO_2 solubility in ILs, mainly because of the low solubilities of H_2 and CO in ILs especially at low pressures. In this case, small apparent absolute values between the experimental and calculated results may result in large ARDs.

We measured the solubility of H_2 in three common pure ILs, that is, $[EMIM]^+[BF_4]^-$, $[BMIM]^+[BF_4]^-$, and $[OMIM]^+[Tf_2N]^-$, as well as in the binary mixed ILs of $[EMIM]^+[BF_4]^-$ (2) + $[OMIM]^+[Tf_2N]^-$ (3) and $[BMIM]^+[BF_4]^-$ (2) + $[OMIM]^+[Tf_2N]^-$ (3) with different mass fractions ($w_3 = 0.2$, 0.5, and 0.8 on a H_2-free basis) at temperatures of 313.2 and 333.2 K. The solubility data and the predicted results are shown in Figures 3 and 4, indicating that H_2 solubility in pure ILs follows the order $[EMIM]^+[BF_4]^- < [BMIM]^+[BF_4]^- < [OMIM]^+[Tf_2N]^-$ at the same operating conditions. Moreover, the results predicted by the UNIFAC model and the experimental data exhibit similar trends and agree very well. The ARDs between the predicted and experimental data are 7.72%, 10.29%, and 4.65% for $[EMIM]^+[BF_4]^-$, $[BMIM]^+[BF_4]^-$, and $[OMIM]^+[Tf_2N]^-$, respectively. Furthermore, the UNIFAC model has a strong power for predicting the solubility of H_2 in two types of binary mixed ILs, with ARDs of 4.64% for the $[EMIM]^+[BF_4]^-$ + $[OMIM]^+[Tf_2N]^-$ mixture and 4.80% for the $[BMIM]^+[BF_4]^-$ + $[OMIM]^+[Tf_2N]^-$ mixture. The detailed values are listed in Supporting Information Tables S6 and S7.

Structure–property relation for IL/CO (H_2) systems

One of the most important applications of the UNIFAC model is to identify the structure–property relation between the molecular structure of ILs and its impact on the separation performance, for example, solubility and selectivity. The Henry's constant[65] on the mole fraction basis was used to

Table 4. Henry's Constant of H_2 in ILs Determined Experimentally (H_{exp}) and Predicted by UNIFAC (H_{pre}) at Different Temperatures (the Values in Parenthesis Come from the Lever Rule)

ILs	T (K)	H_{exp} (MPa)	H_{pre} (MPa)	RD
$[EMIM]^+[BF_4]^-$	313.2	238.42	218.01	0.0856
	333.2	223.18	211.68	0.0515
20 wt % $[EMIM]^+[BF_4]^-$ + 80 wt % $[OMIM]^+[Tf_2N]^-$	313.2	154.50	152.09 (162.43)	0.0156 (0.0513)
	333.2	141.30	145.93 (156.64)	0.0328 (0.1086)
50 wt % $[EMIM]^+[BF_4]^-$ + 50 wt % $[OMIM]^+[Tf_2N]^-$	313.2	182.61	181.83 (191.86)	0.0043 (0.0507)
	333.2	170.33	175.02 (185.79)	0.0275 (0.0908)
80 wt % $[EMIM]^+[BF_4]^-$ + 20 wt % $[OMIM]^+[Tf_2N]^-$	313.2	211.92	205.99 (209.62)	0.0280 (0.0109)
	333.2	203.92	199.14 (203.38)	0.0234 (0.0026)
$[OMIM]^+[Tf_2N]^-$	313.2	124.43	129.06	0.0372
	333.2	120.15	123.59	0.0286
20 wt % $[BMIM]^+[BF_4]^-$ + 80 wt % $[OMIM]^+[Tf_2N]^-$	313.2	138.92	139.27 (140.70)	0.0025 (0.0128)
	333.2	121.75	134.27 (135.42)	0.1028 (0.1123)
50 wt % $[BMIM]^+[BF_4]^-$ + 50 wt % $[OMIM]^+[Tf_2N]^-$	313.2	153.28	152.07 (151.96)	0.0079 (0.0086)
	333.2	136.13	146.54 (146.84)	0.0765 (0.0787)
80 wt % $[BMIM]^+[BF_4]^-$ + 20 wt % $[OMIM]^+[Tf_2N]^-$	313.2	164.19	160.02 (159.25)	0.0254 (0.0301)
	333.2	149.53	154.75 (154.25)	0.0349 (0.0316)
$[BMIM]^+[BF_4]^-$	313.2	177.03	162.84	0.0802
	333.2	167.60	157.89	0.0579

evaluate the absorption ability of various ILs, and it is defined as

$$H_i(T)=\lim_{x_i\to 0}\frac{y_i P\phi_i(T,P,y_i)}{x_i}=\lim_{x_i\to 0}\gamma_i P_i^s(T)=\gamma_i^\infty P_i^s(T) \quad (4)$$

where $\phi_i(T,P,y_i)$ is the fugacity coefficient of gas i in the gas phase, as calculated from the PR equation; γ_i^∞ is the activity coefficient of gas i in the IL at infinite dilution, which can be predicted by the UNIFAC model; P_i^s is the saturated vapor pressure calculated via the extrapolated Antoine equation. The Henry's constants of CO (H_2) in different ILs as previously mentioned were estimated by linear extrapolation at $x_i\to 0$ from the ratio of the fugacity to the mole fraction, and the results together with the predicted data predicted by the UNFAC model using the activity coefficient at infinite dilution, are given in Tables 3 and 4. Notably, the Henry's constants of CO (H_2) in mixed ILs lie between those in pure ILs, which can be estimated by the following lever rule:

$$H_1=X_2H_{1,2}+X_3H_{1,3} \quad (5)$$

where X_2 and X_3 are the mole fractions on a gas-free basis of individual ILs in mixed ILs, and $H_{1,2}$ and $H_{1,3}$ are Henry's constants of gas in individual ILs at the same temperature, as predicted by the UNIFAC model.

The results predicted by Eq. 5 are also given inside parenthesis in Tables 3 and 4. The ARDs of Henry's constants for CO in the mixed ILs are 11.25% and 9.91% for the UNIFAC model and lever rule, respectively, whereas for H_2 they are 3.18% and 4.91%, respectively. These results indicate that both the UNIFAC model and the lever rule suffice for predicting the Henry's constants of CO (H_2) in mixed ILs from high to low temperatures; however, the UNIFAC model appears to be more convenient for routine use.

The selectivity ($S_{i/j}$) of gas i to gas j was used to evaluate the separation selectivity for various ILs, which is defined as

$$S_{i/j}=\frac{H_i(T)}{H_j(T)} \quad (6)$$

Only the selectivity of CO (H_2) to CO_2 is addressed in this work. When Eq. 6 is used, the Henry's constants of CO_2 in ILs are derived from the literature,[3,27,35,37,39,45,46,49,65–69] whereas some data related to CO and H_2 in ILs were extracted from the literature[20,21,23,24,27,29–31,36,37,39] and the others originate from this work. The detailed values and the

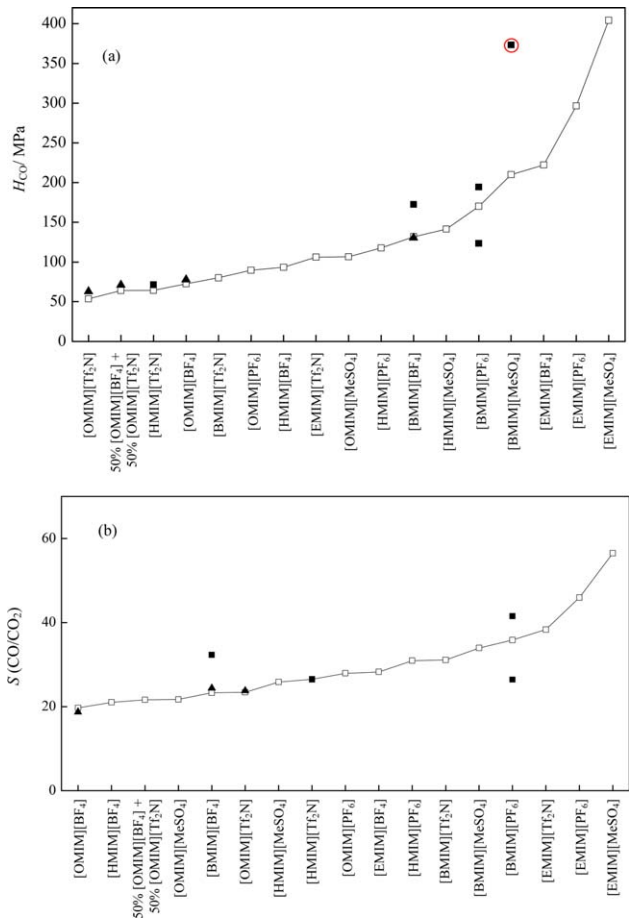

Figure 5. Henry's constant of CO (a) and selectivity of CO to CO_2 (b) in ILs at $T = 293.2$ K.

(□) Results predicted by the UNIFAC model; (■) experimental data from the literature; (▲) experimental data obtained in this work. [Color figure can be viewed in the online issue, which is available at wileyonlinelibrary.com.]

corresponding literature are listed in Supporting Information Table S8. Notably, in an actual mixture, the presence of the second gas will definitely affect the solubility of the first gas in the IL. Therefore, the selectivity ($S_{i/j}$) stated here is an "idealized" selectivity. The interactions between different types of gases are not considered in the current work.

Figure 5 shows the comparison between the experimental data and the UNIFAC predicted results for Henry's constants of CO and the selectivity of CO to CO_2 in various ILs at 293.2 K. Both the experimental and predicted results agree well, except for one group of experimental data[29] marked with red circle. This outlier group is mainly due to the experimental error introduced by the fact that the literature-reported CO solubility in $[BMIM]^+[MeSO_4]^-$ increases with increasing temperature. This result is contradictory to the conclusions for other ILs made by most researchers. Thus, a large deviation is observed for this IL. In addition, by comparison of Figures 5a,b, it can be seen that the Henry's constants of CO and the selectivity of CO to CO_2 in ILs roughly exhibit the same trend, that is, the ILs with a large CO solubility usually have a small selectivity of CO to CO_2.

Figure 6 shows the comparison between the experimental data and the UNIFAC predicted values for the Henry's constants of H_2 and the selectivity of H_2 to CO_2 in various ILs at 333.2 K. It can be seen that both the experimental and predicted results agree well, except for two data points marked with red circles. Increasing the number of carbon atoms in the alkyl chain on cation of an IL will increase the solubility of H_2 in ILs. Notably, for both CO/CO_2 and H_2/CO_2 gas pairs, both the Henry's constants and the selectivity in mixed ILs lie between those in pure ILs.

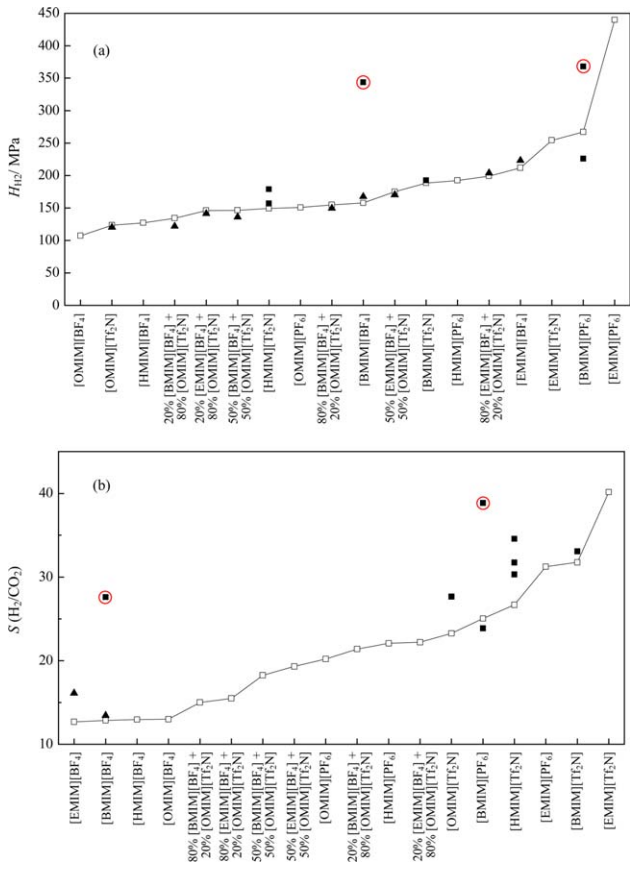

Figure 6. Henry's constant of H_2 (a) and selectivity of H_2 to CO_2 (b) in ILs at $T = 333.2$ K.

(□) Results predicted by the UNIFAC model; (■) experimental data from the literature; (▲) experimental data obtained in this work. [Color figure can be viewed in the online issue, which is available at wileyonlinelibrary.com.]

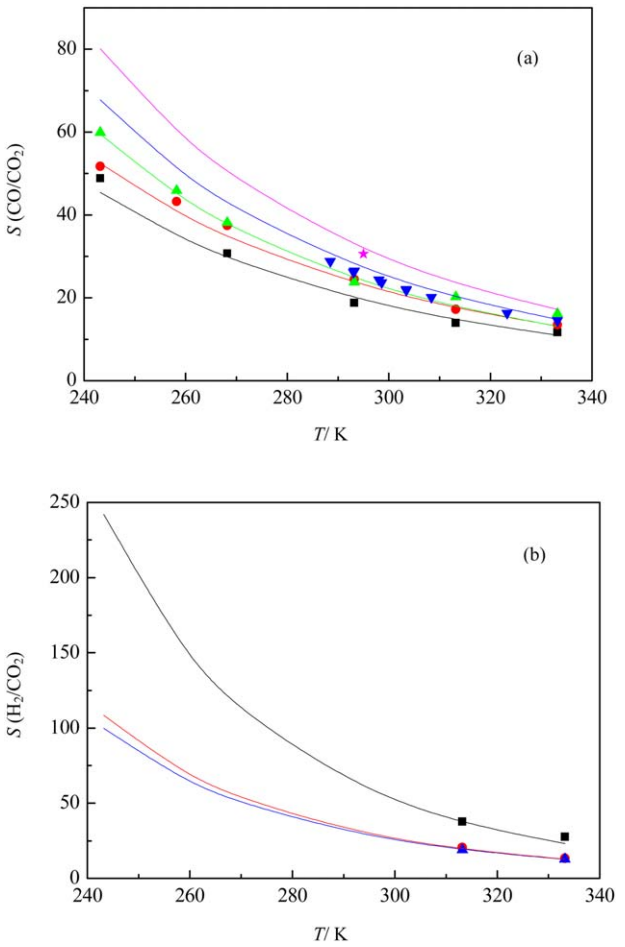

Figure 7. Influence of temperature on selectivity of CO to CO_2 (a) and H_2 to CO_2 (b) in ILs.

Solid lines, results predicted by the UNIFAC model; scattered points, experimental data. (a) (■) [OMIM][BF_4]; (●) $[BMIM]^+[BF_4]^-$; (▲) $[OMIM]^+[Tf_2N]^-$; (▼) $[HMIM]^+[Tf_2N]^-$; (★) $[BMIM]^+[Tf_2N]^-$. (b) (■) $[OMIM]^+[Tf_2N]^-$; (●) $[BMIM]^+[BF_4]^-$; (▲) $[EMIM]^+[BF_4]^-$. [Color figure can be viewed in the online issue, which is available at wileyonlinelibrary.com.]

We went one step further to investigate the influence of temperature on the selectivity of CO (H_2) to CO_2. As shown in Figure 7, a low temperature is not only favorable for increasing the selectivity of both CO/CO_2 and H_2/CO_2 gas pairs but also for increasing the CO_2 solubility. Meanwhile, at the same temperature the selectivity of H_2 to CO_2 is much higher than that of CO to CO_2, indicating that CO/CO_2 are more difficult to separate in comparison with the H_2/CO_2 gas pair, which should be considered in process simulations and optimizations.

Conclusions

This is the first work to extend the familiar UNIFAC model to IL-CO and IL-H_2 systems, and some new group

binary interaction parameters (α_{mn} and α_{nm}) are added into the current UNIFAC parameter matrix via correlation of the solubility data exhaustively collected from the literature at different temperatures and pressures. To test the applicability of the UNIFAC model to predict the solubility of CO (H_2) in pure and mixed ILs at high and low temperatures, we measured the solubility data of CO and H_2 at temperatures from 243.2 to 333.2 K in some common ILs and in their binary mixtures. This work demonstrates the strong predictive power of the UNIFAC model for IL-CO and IL-H_2 systems in both pure and mixed ILs at both high and low temperatures.

Moreover, both the solubility and selectivity of CO (H_2) to CO_2 in various ILs were investigated. It was found that CO solubility exhibits a reverse trend with respect to the selectivity of CO to CO_2, whereas H_2 solubility exhibits a similar trend with the selectivity of H_2 to CO_2. In any event, the selectivity of CO/CO_2 and H_2/CO_2 gas pairs always increases with decreasing temperature. The results of this work will help predict the quantitative thermodynamic behavior of IL-gas systems in gas separation over a wide temperature range.

Acknowledgments

This work was financially supported by the National Nature Science Foundation of China under Grants Nos. 21476009 and 21406007 and by the Chinese Universities Scientific Fund (ZY1401).

Literature Cited

1. Paulechka YU, Zaitsau DH, Kabo GJ, Strechan AA. Vapor pressure and thermal stability of ionic liquid 1-butyl-3-methylimidazolium bis(trifluoromethylsulfonyl)amide. *Thermochim Acta*. 2005;439:158–160.
2. Earle MJ, Seddon KR. Ionic liquids. Green solvents for the future. *Pure Appl Chem*. 2000;72:1391–1398.
3. Finotello A, Bara JE, Camper D, Noble RD. Room-temperature ionic liquids: temperature dependence of gas solubility selectivity. *Ind Eng Chem Res*. 2008;47:3453–3459.
4. Jalili A, Safavi M, Ghotbi C, Mehdizadeh A, Hosseini-Jenab M, Taghikhani V. Solubility of CO_2, H_2S, and their mixture in the ionic liquid 1-octyl-3-methylimidazolium bis(trifluoromethyl)sulfonylimide. *J Phys Chem B*. 2012;116:2758–2774.
5. Brennecke JF, Maginn EJ. Ionic liquids: Innovative fluids for chemical processing. *AIChE J*. 2001;47:2384–2389.
6. Earle MJ, Esperanca JMSS, Gilea MA, Canongia Lopes JN, Rebelo LPN, Magee JW, Seddon KR, Widegren JA. The distillation and volatility of ionic liquids. *Nature*. 2006;439:831–834.
7. Seiler M, Jork C, Kavarnou A, Arlt W, Hirsch R. Separation of azeotropic mixtures using hyperbranched polymers or ionic liquids. *AIChE J*. 2004;50:2439–2454.
8. Lei Z, Dai C, Chen B. Gas solubility in ionic liquids. *Chem Rev*. 2014;114:1289–1326.
9. Shiflett MB, Yokozeki A. Chemical absorption of sulfur dioxide in room-temperature ionic liquids. *Ind Eng Chem Res*. 2010;49:1370–1377.
10. Muldoon MJ, Aki SNVK, Anderson JL, Dixon JK, Brennecke JF. Improving carbon dioxide solubility in ionic liquids. *J Phys Chem B*. 2007;111:9001–9009.
11. Bak T, Nowotny J, Rekas M, Sorrell CC. Photo-electrochemical hydrogen generation from water using solar energy. Materials-related aspects. *Int J Hydrogen Energy*. 2002;27:991–1022.
12. Dyson PJ, Laurenczy G, Ohlin CA, Vallance J, Welton T. Determination of hydrogen concentration in ionic liquids and the effect (or lack of) on rates of hydrogenation. *Chem Commun*. 2003;2418–2419.
13. Berger A, de Souza RF, Delgado MR, Dupont J. Ionic liquid-phase asymmetric catalytic hydrogenation: hydrogen concentration effects on enantioselectivity. *Tetrahedron: Asymmetry*. 2001;12:1825–1828.
14. Jessop PG, Ikariya T, Noyori R. Selectivity for hydrogenation or hydroformylation of olefins by hydridopentacarbonylmanganese (1) in supercritical carbon dioxide. *Organometallics*. 1995;14:1510–1513.
15. Franke R, Selent D, Borner A. Applied hydroformylation. *Chem Rev*. 2012;112:5675–5732.
16. Gasification Introduction. Available at: http://www.netl.doe.gov/research/coal/energy-systems/gasification/gasifipedia/syngas-composition; accessed August 8, 2014.
17. The Rectisol® Process. Available at: http://uicgroupecho.wikispaces.com/file/view/B_0308e_Rectisol.pdf.; accessed August 8, 2014.
18. Kohl AL, Nielsen RB. *Gas Purification*, *5th ed*. Houston: Gulf Publishing Company, 1997.
19. Raeissi S, Florusse LJ, Peters CJ. Purification of flue gas by ionic liquids: carbon monoxide capture in [bmim][Tf2N]. *AIChE J*. 2013;59:3886–3891.
20. Ohlin CA, Dyson PJ, Laurenczy G. Carbon monoxide solubility in ionic liquids: determination, prediction and relevance to hydroformylation. *Chem Commun*. 2004;1070–1071.
21. Jacquemin J, Costa Gomes MF, Husson P, Majer V. Solubility of carbon dioxide, ethane, methane, oxygen, nitrogen, hydrogen, argon, and carbon monoxide in 1-butyl-3-methylimidazolium tetrafluoroborate between temperatures 283 K and 343 K and at pressures close to atmospheric. *J Chem Thermodyn*. 2006;38:490–502.
22. Zhao Y, Zhang X, Dong H, Zhen Y, Li G, Zeng S, Zhang S. Solubilities of gases in novel alcamines ionic liquids 2-[2-hydroxyethyl (methyl) amino] ethanol chloride. *Fluid Phase Equilib*. 2011;302:60–64.
23. Kumełan J, Kamps ÁPS, Tuma D, Maurer G. Solubility of CO in the ionic liquid [bmim][PF6]. *Fluid Phase Equilib*. 2005;228–229:207–211.
24. Kumełan J, Kamps ÁPS, Tuma D, Maurer G. Solubility of the single gases carbon monoxide and oxygen in the ionic liquid [hmim][Tf2N]. *J Chem Eng Data*. 2009;54:966–971.
25. Sharma A, Julcour C, Kelkar AA, Deshpande RM, Delmas H. Mass transfer and solubility of CO and H_2 in ionic liquid. Case of [Bmim][PF6] with gas-inducing stirrer reactor. *Ind Eng Chem Res*. 2009;48:4075–4082.
26. Florusse LJ, Raeissi S, Peters CJ. An IUPAC task group study: the solubility of carbon monoxide in [hmim][Tf2N] at high pressures. *J Chem Eng Data*. 2011;56:4797–4799.
27. Jacquemin J, Husson P, Majer V, Costa Gomes MF. Low-pressure solubilities and thermodynamics of solvation of eight gases in 1-butyl-3-methylimidazolium hexafluorophosphate. *Fluid Phase Equilib*. 2006;240:87–95.
28. Urukova I, Vorholz J, Maurer G. Solubility of CO_2, CO, and H_2 in the ionic liquid [bmim][PF6] from Monte Carlo simulations. *J Phys Chem B*. 2005;109:12154–12159.
29. Kumełan J, Kamps ÁPS, Tuma D, Maurer G. Solubility of the single gases H_2 and CO in the ionic liquid [bmim][CH_3SO_4]. *Fluid Phase Equilib*. 2007;260:3–8.
30. Bermejo MD, Fieback TM, Martín Á. Solubility of gases in 1-alkyl-3methylimidazolium alkyl sulfate ionic liquids: experimental determination and modeling. *J Chem Thermodyn*. 2013;58:237–244.
31. Kumełan J, Kamps ÁPS, Tuma D, Maurer G. Solubility of H_2 in the ionic liquid [bmim][PF6]. *J Chem Eng Data*. 2006;51:11–14.
32. Kumełan J, Kamps ÁPS, Tuma D, Maurer G. Solubility of H_2 in the ionic liquid [hmim][Tf2N]. *J Chem Eng Data*. 2006;51:1364–1367.
33. Kumełan J, Tuma D, Kamps ÁPS, Maurer G. Solubility of the single gases carbon dioxide and hydrogen in the ionic liquid [bmpy][Tf2N]. *J Chem Eng Data*. 2010;55:167–172.
34. Raeissi S, Peters CJ. Understanding temperature dependency of hydrogen solubility in ionic liquids, including experimental data in [bmim][Tf2N]. *AIChE J*. 2012;58:3553–3559.
35. Afzal W, Liu X, Prausnitz JM. Solubilities of some gases in four immidazolium-based ionic liquids. *J Chem Thermodyn*. 2013;63:88–94.
36. Raeissi S, Florusse LJ, Peters CJ. Hydrogen solubilities in the IUPAC ionic liquid 1-hexyl-3-methylimidazolium bis(trifluoromethylsulfonyl)imide. *J Chem Eng Data*. 2011;56:1105–1107.
37. Jacquemin J, Husson P, Majer V, Costa Gomes MF. Influence of the cation on the solubility of CO_2 and H_2 in ionic liquids based on the bis(trifluoromethylsulfonyl)imide anion. *J Solution Chem*. 2007;36:967–979.
38. Raeissi S, Schilderman AM, Petersb CJ. High pressure phase behaviour of mixtures of hydrogen and the ionic liquid family [cnmim][Tf2N]. *J Supercrit Fluids*. 2013;73:126–129.
39. Costa Gomes MF. Low-pressure solubility and thermodynamics of solvation of carbon dioxide, ethane, and hydrogen in 1-hexyl-3-

methylimidazolium bis(trifluoromethylsulfonyl)amide between temperatures of 283 K and 343 K. *J Chem Eng Data*. 2007;52:472–475.
40. Zhou L, Fan J, Shang X, Wang J. Solubilities of CO_2, H_2, N_2 and O_2 in ionic liquid 1-n-butyl-3-methylimidazolium heptafluorobutyrate. *J Chem Thermodyn*. 2013;59:28–34.
41. Yuan X, Zhang S, Chen Y, Lu X, Dai W, Mori R. Solubilities of gases in 1,1,3,3-tetramethylguanidium lactate at elevated pressures. *J Chem Eng Data*. 2006;51:645–647.
42. Manan NA, Hardacre C, Jacquemin J, Rooney DW, Youngs TG. Evaluation of gas solubility prediction in ionic liquids using COSMOthermX. *J Chem Eng Data*. 2009;54:2005–2022.
43. Lei Z, Zhang J, Li Q, Chen B. UNIFAC model for ionic liquids. *Ind Eng Chem Res*. 2009;48:2697–2698.
44. Lei Z, Dai C, Liu X, Xiao L, Chen B. Extension of the UNIFAC model for ionic liquids. *Ind Eng Chem Res*. 2012;51;12135–12144.
45. Lei Z, Dai C, Wang W, Chen B. UNIFAC model for ionic liquid-CO_2 systems. *AIChE J*. 2014;60:716–729.
46. Dai C, Lei Z, Xiao L, Wang W, Chen B. Group contribution lattice fluid equation of state for CO_2—ionic liquid systems: an experimental and modeling study. *AIChE J*. 2013;59:4399–4412.
47. Lei Z, Yuan J, Zhu J. Solubility of CO_2 in propanone, 1-ethyl-3-methylimidazolium tetrafluoroborate, and their mixtures. *J Chem Eng Data*. 2010;55:4190–4194.
48. Lei Z, Qi X, Zhu J, Li Q, Chen B. Solubility of CO_2 in acetone, 1-butyl-3-methylimidazolium tetrafluoroborate, and their mixtures. *J Chem Eng Data*. 2012;57:3458–3466.
49. Lei Z, Han J, Zhang B, Li Q, Zhu J, Chen B. Solubility of CO_2 in binary mixtures of room-temperature ionic liquids at high pressures. *J Chem Eng Data*. 2012;57:2153–2159.
50. Blanchard LA, Hancu D, Beckman EJ, Brennecke JF. Green processing using ionic liquids and CO_2. *Nature*. 1999;399:28–29.
51. Santiago RS, Santos GR, Aznar M. UNIQUAC correlation of liquid-liquid equilibrium in systems involving ionic liquids: the DFT-PCM approach. *Fluid Phase Equilib*. 2009;278:54–61.
52. Banerjee T, Singh MK, Sahoo RK, Khanna A. Volume, surface and UNIQUAC interaction parameters for imidazolium based ionic liquids via polarizable continuum model. *Fluid Phase Equilib*. 2005; 234:64–76.
53. Scientific Computing & Modeling. Available at: http://www.scm.com/Doc/Doc2010/CRS/CRS/page18.html.; accessed August 8, 2014.
54. Diedenhofen M, Klamt A. COSMO-RS as a tool for property prediction of IL mixtures-a review. *Fluid Phase Equilib*. 2010;294:31–38.
55. Fogg PGT, Gerrard W. *Solubility of Gases in Liquids: A Critical Evaluation of Gas/Liquid Systems in Theory and Practice*. New York: Wiley, 1991.
56. Kim Y, Choi W, Jang J, Yoo K, Lee C. Solubility measurement and prediction of carbon dioxide in ionic liquids. *Fluid Phase Equilib*. 2005;228–229:439–445.
57. Kim JE, Lim JS, Kang JW. Measurement and correlation of solubility of carbon dioxide in 1-alkyl-3-methylimidazolium hexafluorophosphate ionic liquids. *Fluid Phase Equilib*. 2011;306:251–255.
58. Breure B, Bottini SB, Witkamp GJ, Peters CJ. Thermodynamic modeling of the phase behavior of binary systems of ionic liquids and carbon dioxide with the group contribution equation of state. *J Phys Chem B*. 2007;111:14265–14270.
59. Bermejo MD, Martin A, Foco G, Cocero MJ, Bottini SB, Peters CJ. Application of a group contribution equation of state for the thermdynamic modeling of the binary systems CO2-1-butyl-3-methyl imidazolium nitrate and CO2-1-hydroxy-1-methyl imidazolium nitrate. *J Supercrit Fluids*. 2009;50:112–117.
60. Dong L, Zheng D, Wu X. Working pair selection of compression and absorption hybrid cycles through predicting the activity coefficients of hydrofluorocarbon + ionic liquid systems by the UNIFAC model. *Ind Eng Chem Res*. 2012;51:4741–4747.
61. Yunus NM, Abdul Mutalib MI, Murugesan T. Modeling of solubility of CO_2 in 1-butylpyridinium bis(trifluoromethylsulfonyl)imide ionic liquid using UNIFAC. *AIP Conf Proc*. 2012;1482:229–233.
62. Gmehling J, Rasmussen P, Fredenslund A. Vapor-liquid equilibria by UNIFAC group contribution. 2. Revision and extension. *Ind Eng Chem Process Des Dev*. 1982;21:118–127.
63. Kleiber M. An extension to the UNIFAC group assignment for prediction of vapor-liquid equilibria of mixtures containing refrigerants. *Fluid Phase Equilib*. 1995;107:161–188.
64. Palgunadi J, Kang JE, Nguyen DQ, Kim JH, Min BK, Lee SD, Kim H, Kim HS. Solubility of CO_2 in dialkylimidazolium dialkylphosphate ionic liquids. *Thermochim Acta*. 2009;494:94–98.
65. Lee BC, Outcalt SL. Solubilities of gases in the ionic liquid 1-n-butyl-3-methylimidazolium bis(trifluoromethylsulfonyl)imide. *J Chem Eng Data*. 2006;51:892–897.
66. Hou Y, Baltus RE. Experimental measurement of the solubility and diffusivity of CO_2 in room-temperature ionic liquids using a transient thin-liquid-film method. *Ind Eng Chem Res*. 2007;46:8166–8175.
67. Zhang J, Zhang Q, Qiao B, Deng U. Solubilities of the gaseous and liquid solutes and their thermodynamics of solubilization in the novel room-temperature ionic liquids at infinite dilution by gas chromatography. *J Chem Eng Data*. 2007;52:2277–2283.
68. Baltus RE, Culbertson BH, Dai S, Luo H, DePaoli DW. Low-pressure solubility of carbon dioxide in room temperature ionic liquids measured with a quartz crystal microbalance. *J Phys Chem B*. 2004; 108:721–727.
69. Chen Y, Zhang S, Yuan X, Zhang Y, Zhang X, Dai W, Mori R. Solubility of CO_2 in imidazolium-based tetrafluoroborate ionic liquids. *Thermochim Acta*. 2006;441:42–44.
70. Anthony JL, Anderson JL, Maginn EJ, Brennecke JF. Anion effects on gas solubility in ionic liquids. *J Phys Chem B*. 2005;109:6366–6374.
71. Aki SNVK, Mellein BR, Saurer EM, Brennecke JF. High-pressure phase behavior of carbon dioxide with imidazolium-based ionic liquids. *J Phys Chem B*. 2004;108:20355–20365.

Manuscript received Dec. 14, 2013, and revision received Aug. 8, 2014.